Identification of potential key genes and functional role of CENPF in osteosarcoma using bioinformatics and experimental analysis

YIHUI MA[1], JIAPING GUO[1], DA LI[1] and XIANHUA CAI[2]

Departments of [1]Stomatology and [2]Orthopedics, General Hospital of Central Theater Command of The People's Liberation Army, Wuhan, Hubei 430070, P.R. China

Received January 14, 2020; Accepted September 21, 2021

DOI: 10.3892/etm.2021.11003

Abstract. Osteosarcoma, which arises from bone tissue, is considered to be one of the most common types of cancer in children and teenagers. As the etiology of osteosarcoma has not been fully elucidated, the overall prognosis for patients is generally poor. In recent years, the development of bioinformatical technology has allowed researchers to identify numerous molecular biological characteristics associated with the prognosis of osteosarcoma using online databases. In the present study, Gene Expression Omnibus (GEO) database was used and three microarray datasets were obtained. The GEO2R web tool was utilized and differentially expressed genes (DEGs) in osteosarcoma tissue were identified. Venn analysis was performed to determine the intersection of the DEG profiles. DEGs were analyzed by Gene Ontology function and Kyoto Encyclopedia of Genes and Genomes pathway enrichment analysis. Protein-protein interactions (PPIs) between these DEGs were analyzed using the Search Tool for the Retrieval of Interacting Genes database, and the PPI network was then visualized using Cytoscape software. The top ten genes were identified based on measurement of degree, density of maximum neighborhood component, maximal clique centrality and mononuclear cell counts in the PPI network, and five overlapping genes [origin recognition complex subunit 6 (ORC6), IGF-binding protein 5 (IGFBP5), minichromosome maintenance 10 replication initiation factor (MCM10), MET proto-oncogene, receptor tyrosine kinase (MET) and centromere protein F (CENPF)] were identified. Additionally, three module networks were analyzed by Molecular Complex Detection (MCODE), and six key genes [ORC6, MCM10, DEP domain containing 1 (DEPDC1), CENPF, TIMELESS interacting protein (TIPIN) and shugoshin 1 (SGOL1)] were screened. Combined with the results from Cytoscape and MCODE, eight hub genes (ORC6, MCM10, DEPDC1, CENPF, TIPIN, SGOL1, MET and IGFBP5) were obtained. Furthermore, Kaplan-Meier plotter survival analysis was used to evaluate the prognostic value of these eight hub genes in patients with osteosarcoma. Oncomine and GEPIA databases were applied to further confirm the expression levels of hub genes in tissue. Finally, the functional roles of the core gene CENPF were investigated using Cell Counting Kit-8, wound healing and Transwell assays, which indicated that CENPF knockdown inhibited the proliferation, migration and invasion of osteosarcoma cells. These results provided potential prognostic markers, as well as a basis for further investigation of the mechanism underlying osteosarcoma.

Introduction

Osteosarcoma is the most common tumor of bone and derives from primitive bone-forming mesenchymal cells (1,2). Patients with advanced osteosarcoma fail to respond to conventional treatments, such as surgical resection, chemoradiation followed by neoadjuvant chemotherapy and local radiotherapy (3,4). Therefore, the prognosis for the majority of patients with osteosarcoma is poor (5,6). Notably, researchers have discovered certain molecular targets associated with osteosarcoma (7-12). Further promising tumor molecular targets remain to be investigated.

Gene Expression Omnibus (GEO) (13) is a public functional genomics data repository of high throughout gene expression data, chips and microarrays. Microarray and bioinformatics analyses have been widely used to screen genetic alterations in various types of tumor, such as breast cancer and follicular lymphoma (14-16). In addition, gene expression level signatures and biological processes are identified using microarray and bioinformatics analyses (17,18). Moreover, promising targets for tumors have also been distinguished. For example, researchers identified the role of microRNA (miR)-101-3p and its functional role in hepatocellular carcinoma using bioinformatics (19); Zhou *et al* (20) screened 15 hub genes and pathways to identify potential prognostic markers for hepatocellular carcinoma treatment using bioinformatics analysis (20). Integrative bioinformatics have identified links

Correspondence to: Professor Xianhua Cai, Department of Orthopedics, General Hospital of Central Theater Command of the People's Liberation Army, 627 Wuluo Road, Wuchang, Wuhan, Hubei 430070, P.R. China
E-mail: wgcaixh@163.com

Key words: bioinformatics analysis, osteosarcoma, hub genes, centromere protein F, migration

between HNF1 homeobox B with clear cell carcinoma and tumor-associated thrombosis (21), and long non-coding RNA HOXA11-antisense RNA has been demonstrated to have clinical relevance and effects in non-small cell lung cancer (22).

In the present study, bioinformatics analyses were performed to elucidate new targets to provide novel therapeutic targets for the treatment of osteosarcoma In order to select differentially expressed genes (DEGs) in osteosarcoma tissue, gene expression level profiling data was downloaded from the Gene Expression Omnibus (GEO) database. Secondly, Gene Ontology (GO) functional annotation analysis and Kyoto Encyclopedia of Genes and Genomes (KEGG) pathway enrichment analysis were performed for the screened DEGs. Subsequently, a protein-protein interaction (PPI) network was established and Cytoscape software was applied to select hub genes associated with osteosarcoma. Survival analysis of these hub genes was performed using the online database Kaplan-Meier plotter. Oncomine and Gene Expression Profiling Interactive Analysis (GEPIA) databases were used to further confirm the expression levels of hub genes. Notably, a series of functional experiments indicated that knockdown of the core gene centromere protein F (CENPF) suppressed proliferation, migration and invasion in osteosarcoma cell lines.

Materials and methods

Microarray data. Using the GEO database (ncbi.nlm.nih.gov/geo/), three gene expression level profiles [GSE37552 (23), GSE9508 (24) and GSE19357] were selected based on the platforms GPL570 [(HG-U133_Plus_2) Affymetrix Human Genome U133 Plus 2.0 Array], GPL6076 (Agilent-Whole Human Genome Oligo Microarray G4112A condensed) and GPL6244 (HuGene-1_0-st) Affymetrix Human Gene 1.0 ST Array [transcript (gene) version], respectively.

DEGs profiles. Using the GEO2R (25) online analysis tool (ncbi.nlm.nih.gov/geo/geo2r/), DEGs were identified between osteosarcoma and normal tissue. The DEGs were calculated with thresholds of $P<0.05$ and $|\log \text{fold-change (FC)}|>1.00$. Intersections between each dataset were obtained using the Venn diagram tool (bioinformatics.psb.ugent.be/webtools/Venn/).

Functional and pathway enrichment analysis. GO (26) annotations were downloaded from GO. KEGG (27) pathway enrichment analysis of DEGs was applied to determine enriched signaling pathways. Metascape tool (metascape.org/gp/index.html) was used for annotation. $P<0.01$ and gene count >3 were considered to indicate a statistically significant result.

Hub genes selection. A PPI network was constructed using STRING (V11.5, Swiss) database (https:string-db.org/). Visualization of PPI networks was performed using Cytoscape software (V3.7.2, BioStar team; https://apps.cytoscape.org/apps/mcode). Hub genes from DEGs were further defined according to module connectivity in the PPI network. Highly interconnected nodes indicated greater essential connectivity. CytoHubba (28) add-on to the aforementioned Cytoscape was used to determine the connectivity of each node measured by degree, density of maximum neighborhood component (DMNC), maximal clique centrality (MCC) and mononuclear cell counts (MNC).

Molecular Complex Detection (MCODE) analysis. A Cytoscape plugin, MCODE (29), was used to identify significant molecular complexes in the PPI network. Corresponding networks of gene modules were annotated using the UniProt database (uniprot.org/).

Survival analysis of hub genes. Clinical and gene expression level data were analyzed using the Kaplan-Meier plotter (kmplot.com/analysis/) database. The prognostic values of hub genes were analyzed in patients with osteosarcoma. All cases were grouped according to the median value of mRNA expression levels. $P<0.05$ was considered to indicate a statistically significant difference.

GEPIA and Oncomine database for data validation. GEPIA (gepia.cancer-pku.cn/), was applied to analyze RNA sequencing expression level data. The Oncomine (oncomine.org/resource/main.html) database was used to confirm the expression levels of the eight hub genes.

Cell culture. Osteosarcoma cell lines MG-63 and U-2OS were obtained from Cell Resource Center, Shanghai Institutes for Biological Sciences at the Chinese Academy of Sciences. The MG-63 cells and U-2OS cells were cultured in minimal essential medium (MEM) and McCoy's 5A medium (Hyclone; Cytiva), respectively, supplemented with 10% FBS (Gibco; Thermo Fisher Scientific, Inc.), 1% penicillin and streptomycin (Hyclone; Cytiva) under a controlled atmosphere with 5% CO_2 at 37˚C and relative humidity of 85-95%.

Reverse transcription-quantitative PCR (RT-qPCR). Total RNA in cells was extracted using TRIzol® reagent (Invitrogen; Thermo Fisher Scientific, Inc.). The concentration of RNA samples was then measured using a spectrophotometer. Total RNA was reverse-transcribed into first-strand complementary DNA using a Primescript RT reagent kit according to the manufacturer's protocol (Takara Bio, Inc.). For qPCR, 2X SYBR Green qPCR Master Mix (Suzhou Yuheng Biological Technology Co., Ltd.) was used on an ABI 7900 system (Applied Biosystems; Thermo Fisher Scientific, Inc.). The primer sequences used were as follows: CENPF forward, 5'-CGTCCCCGAGAGCAAGTTTATT-3', and reverse, 5'-ACTGCCTTTGCTGCTTTTCC-3'; GAPDH forward, 5'-GCTCTCTGCTCCTCCTGTTC-3', and reverse, 5'-CGACCAAATCCGTTGACTCC-3'. Amplification conditions were as follows: 95˚C for 30 sec, followed by 40 cycles at 95˚C for 15 sec and 60˚C for 45 sec. The relative change in mRNA expression levels was calculated according to the $2^{-\Delta\Delta Cq}$ method (30).

Transfection. Small interfering (si)RNA1 (si-CENPF-1), siRNA2 (si-CENPF-2) and negative control (NC) siRNA (non-targeting sequence) were purchased from Sangon Biotech Co., Ltd. MG-63 and U-2OS cells were incubated

at 37˚C with 5% CO_2 for 24 h, and subsequently plated and transfected with 3.125 nm of si-NC, si-CENPF-1 or si-CENPF-2 at a density of 3,000 cells/well for use in the CCK-8 assay. Moreover, a total of $1x10^5$ cells/well were plated and transfected with 50 nm si-NC, si-CENPF-1 or si-CENPF-2 for the wound healing and Transwell assays. All transfections were carried out using LipoHigh transfection reagent (Sangon Biotech Co., Ltd.) for 4 h after plated for 16-24 h. The cells were collected after 48 h for use in subsequent experiments. The sequences were as follows: siRNA NC, 5'-TTCTCCGAACGTGTCACGTdTdT-3'; si-CENPF-1 (Sense), 5'-GCAGAATCTTAGTAGTCAA-3'; and si-CENPF-2 (sense), 5'-GCAACCATCTACTTGAAGA-3'. The level of transfection efficiency was higher for si-CENPF-2 compared with that of si-CENPF-1, and it was therefore selected for subsequent assays.

Western blotting. The protein expression levels of CENPF were detected by western blotting. The transfected MG-63 and U-2OS cells were washed with pre-cooled PBS on ice and then boiled for 10 min in SDS-sample buffer (Beyotime Institute of Biotechnology). The concentration of protein was determined using a BCA assay according to the manufacturer's instructions (Sangon Biotech Co., Ltd.), and the absorbance was read at 570 nm using Thermo Multiskan FC (version, US6111636; Thermo Fisher Scientific, Inc.). A total of 30 μg protein lysates/per lane were separated by electrophoresis with 10% SDS-PAGE. Afterwards, the samples were transferred to PVDF membranes. Membranes were blocked for 1 h with 5% skimmed milk at room temperature, and then incubated at 4˚C overnight with the following primary antibodies from ABclonal Biotech Co., Ltd.: GAPDH (1:1,000; cat. no. AC002) and CENPF (1:1,000; cat. no. A18644). Subsequently, membranes were incubated at 37˚C for 1 h with the GAPDH HRP goat anti-mouse IgG (1:10,000; cat. no. AS003) and CENPF goat anti-rabbit IgG (1:10,000; cat. no. AS014) secondary antibodies from ABclonal Biotech Co., Ltd. Bands were visualized using chemiluminescence HRP Substatet (MilliporeSigma). The Bio-Rad gel Doc XR + system (Bio-Rad Laboratories, Inc.) was used to scan the gel images. ImageJ (version, 1.53e; National Institutes of Health) was used for grayscale analysis. GAPDH was used as an internal control.

Cell proliferation assay. Cell Counting Kit-8 (CCK-8) assays (Beyotime Institute of Biotechnology) were performed according to the manufacturer's protocol. MG-63 and U-2OS cells were seeded in 96-well plates at a density of 3,000 cells/well and transfected at 16-24 h, and subsequently cultured at 37˚C in a 5% CO_2 incubator. CCK-8 was added to each well at 0, 24, 48 and 72 h after transfection. Following incubation for 1 h at 37˚C, the absorbance at 450 nm was read using Thermo Multiskan FC (version, US6111636; Thermo Fisher Scientific, Inc.). A total of three independent repeats were performed.

Wound healing assay. MG-63 and U-2OS cells were seeded in 6-well plates at a density of $1x10^5$ cells/well, cultured for ~16-24 h and transfected. Cells were used at ~80-90% confluence on the day of transfection. LipoHigh transfection reagent

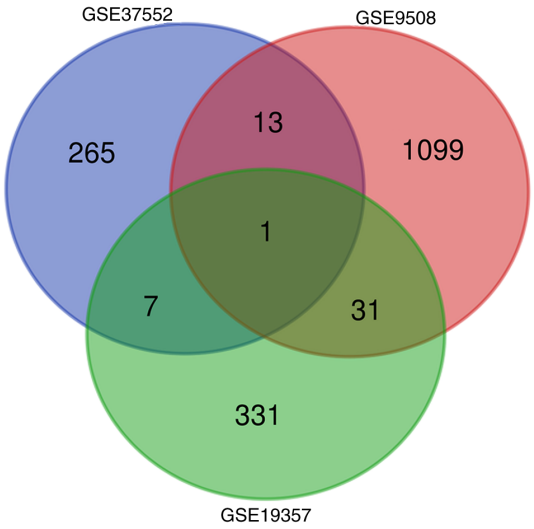

Figure 1. Selection of three gene expression level profiles and identification of DEGs. A total of three gene expression level profiles were selected. In total, 52 DEGs were identified in accordance with the criteria of P<0.05 and |log fold-change|≥1: Seven overlapping genes in GSE37552 and GSE19357; 13 overlapping genes in GSE37552 and GSE9508; 31 overlapping genes in GSE19357 and GSE9508; and one overlapping gene in GSE37552, GSE9508 and GSE19357. In addition, Venn diagram analysis presents the intersection of DEGs. DEG, differentially expressed gene.

(5 μl/well; Sangon Biotech Co., Ltd.) and corresponding RNA (100 pmol/well) were added. After transfection for 4-6 h, cells were uniformly scratched using a sterile pipette, washed with PBS and then respectively cultured in MEM and McCoy's 5A medium (Hyclone; Cytiva) with 2% FBS for 72 h at 37˚C in a 5% CO_2 incubator. The wound images were observed and captured using an optical microscope at (magnification, x40; version, CKX41; Olympus Corporation) at 0, 24, 48 and 72 h. The quantification data for wound closure assay was calculated using the following formula: Distance wound closed=initial wound width-final wound width; wound closure rate=distance wound closed/initial wound width.

Transwell assays. Transwell migration assays were performed, and a total of $1x10^4$ MG-63 and U-2OS cells were seeded into the top chamber in serum-free medium, and medium containing 10% FBS was placed in the bottom chamber. Migrated cells were fixed in 4% polyformaldehyde for 30 min at room temperature, and subsequently stained with 0.1% crystal violet for 20 min at room temperature. Five views per group were selected and images were captured at x100 magnification using a light microscope. A total of three independent repeats was performed.

Transwell invasion assays were also performed using Millipore Transwell chambers. Transfected cells were resuspended in serum-free MEM or McCoy's 5A medium and placed in the upper chamber, previously coated with Matrigel (BD Biosciences) at 37˚C for 6 h, while MEM or McCoy's 5A medium containing 10% FBS was added to the lower chamber. Following incubation for 24 h at 37˚C in a 5% CO_2 incubator, cells in the upper membrane were removed with cotton swabs, whereas invaded cells were fixed in 4% polyformaldehyde for 30 min at room temperature and stained with 0.1% crystal

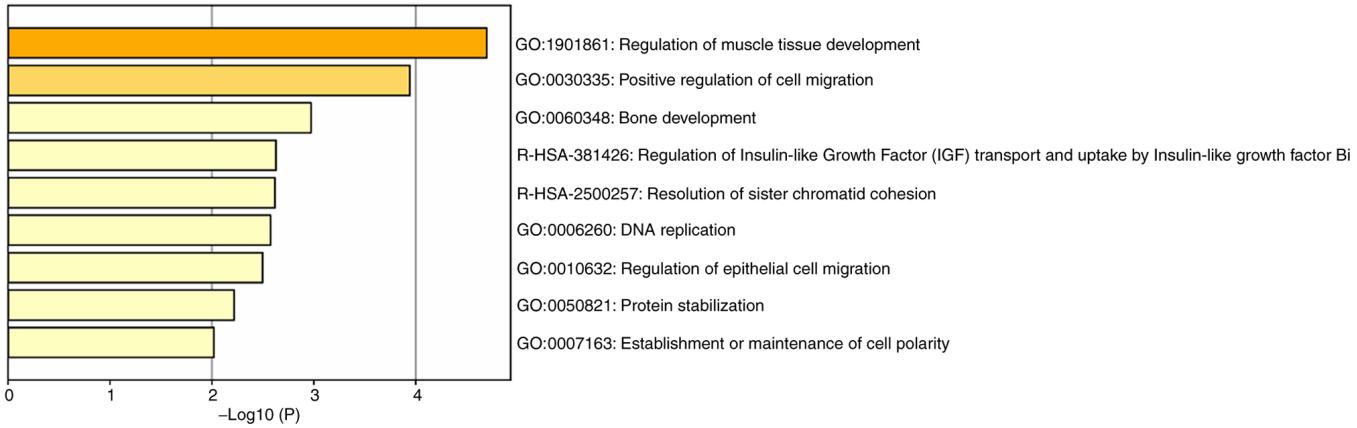

Figure 2. GO term and KEGG enrichment analysis of DEGs. The online analysis tool Metascape was applied to identify GO categories and KEGG pathways for DEGs. The terms 'muscle tissue development', 'cell migration', 'bone development' and 'resolution of sister chromatid cohesion' were primarily enriched with DEGs. GO, Gene Ontology; KEGG, Kyoto Encyclopedia of Genes and Genomes; DEG, differentially expressed gene.

violet for 20 min at room temperature. Five views per group were selected and images were captured at x100 magnification using an optical microscope. A total of three independent repeats was performed.

Statistical analysis. All data were analyzed with GraphPad Prism 7.0 software (GraphPad Software, Inc.) and are expressed as the mean ± standard deviation. Paired student's t-test was used to analyze differences between two groups. One-way ANOVA followed by Dunnett's post hoc multiple comparisons test were used to analyze differences between >2 groups. All experiments were performed in triplicate. $P<0.05$ was considered to indicate a statistically significant difference.

Results

Selection of three gene expression level profiles and identification of DEGs. A total of three gene expression level profiles were selected. GSE37552 consisted of two metastatic samples and two non-metastatic samples; GSE9508 included 13 samples from non-metastatic patients and 21 samples from metastatic patients; GSE19357 contained five frozen bone tumor biopsies (two osteochondromas, two cases of unusual parosteal osteochondromatous proliferation and one subungual exostosis). In total, 52 DEGs were identified in accordance with the criteria of $P<0.05$ and $|logFC|>1$: Seven overlapping genes in GSE37552 and GSE19357; 13 overlapping genes in GSE37552 and GSE9508; 31 overlapping genes in GSE19357 and GSE9508; and one overlapping gene in GSE37552, GSE9508 and GSE19357. Venn diagram analysis presents the intersection of DEGs (Fig. 1). Subsequently, seven overlapping DEGs were selected from three gene expression profiles.

GO term and KEGG enrichment analyses of DEGs. The online analysis tool Metascape was applied to identify GO categories and KEGG pathways for DEGs. The results indicated that the terms 'regulation of muscle tissue development', 'positive regulation of cell migration', 'bone development' and 'resolution of sister chromatid cohesion' were primarily enriched with DEGs (Fig. 2).

Identification of hub genes. Protein interactions between DEGs were determined using STRING in the PPI network. A total of 52 nodes and 80 edges were included (Fig. 3A). Hub genes were identified based on the connectivity of degree, DMNC, MCC and MNC in the PPI network (Fig. 3B). Venn analysis was performed to determine the intersection of the DEG profiles, which indicated that five genes were overlapping in those four analysis methods (degree, DMNC, MCC and MNC; Fig. 3C). Additionally, three module networks were analyzed by MCODE. The most important module with six genes was selected (Fig. 3D). Collectively, the results of the union of set were calculated according to the methods of hub genes selection and eight genes [DEP domain containing 1 (DEPDC1), TIMELESS interacting protein (TIPIN), shugoshin 1 (SGOL1), origin recognition complex subunit 6 (ORC6), IGF-binding protein 5 (IGFBP5), minichromosome maintenance 10 replication initiation factor (MCM10), MET proto-oncogene, receptor tyrosine kinase (MET) and CENPF] were identified. Thus, eight hub genes were obtained using Cytohubba and MCODE analysis.

Survival analysis of hub genes. Kaplan-Meier plotter online database provided the prognostic values of eight hub genes. Overall survival analysis of 259 cases indicated that with the exception of IGFBP5, high expression levels of the hub genes (DEPDC1, TIPIN, SGOL1, ORC6, MCM10, MET and CENPF) were significantly associated with unfavorable overall survival in patients with osteosarcoma (Fig. 4). The survival curve of eight hub genes exhibited significant differences between low and high expression levels.

Confirmation of differential expression level hub genes. In order to confirm the differential hub gene expression levels, expression level profiles were constructed based on GEPIA, which demonstrated that the hub genes ORC6 and CENPF were significantly upregulated in osteosarcoma (Fig. 5A). In order to verify the results, the expression levels of hub genes were

A

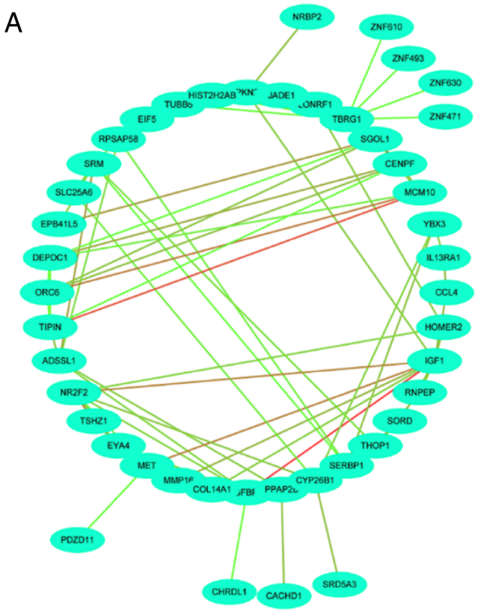

B

Top 10 in network string_interactions. tsv ranked by degree method

Rank	Name	Score
1	IGF1	10
2	IGFBP5	8
2	TBRG1	8
4	NR2F2	7
5	MET	6
5	SRM	6
7	CENPF	5
7	SGOL1	5
7	MCM10	5
7	ORC6	5

Top 10 in network string_interactions. tsv ranked by DMNC method

Rank	Name	Score
1	CENPF	0.583436375
1	MCM10	0.583436375
1	ORC6	0.583436375
1	DEPDC1	0.583436375
5	SGOL1	0.568393712
5	TIPIN	0.568393712
7	MMP16	0.473661427
8	COL14A1	0.463463057
9	MET	0.453783847
10	IGFBP5	0.427942465

Top 10 in network string_interactions. tsv ranked by MCC method

Rank	Name	Score
1	DEPDC1	48
1	ORC6	48
1	MCM10	48
1	CENPF	48
5	IGFBP5	26
6	TIPIN	25
6	SGOL1	25
8	IGF1	24
9	MET	19
10	NR2F2	17

Top 10 in network string_interactions. tsv ranked by MNC method

Rank	Name	Score
1	NR2F2	6
1	IGFBP5	6
1	IGF1	6
4	MET	5
4	DEPDC1	5
4	ORC6	5
4	MCM10	5
4	CENPF	5
9	MMP16	4
9	EYA4	4

C

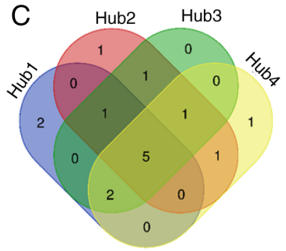

Names	Total	Elements
Hub1 Hub2 Hub3 Hub4	5	ORC6 IGFBP5 MCM10 MET CENPF
Hub1 Hub2 Hub3	1	SGOL1
Hub1 Hub3 Hub4	2	IGF1 NR2F2
Hub2 Hub3 Hub4	1	DEPDC1
Hub2 Hub3	1	TIPIN
Hub2 Hub4	1	MMP16
Hub1	2	SRM TBRG1
Hub2	1	COL14A1
Hub4	1	EYA4

D

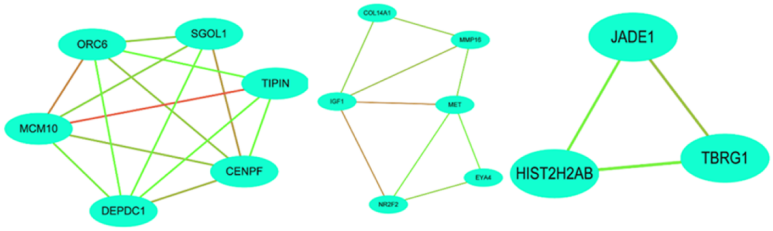

Figure 3. Identification of hub genes. (A) Protein interactions between DEGs were determined using Search Tool for the Retrieval of Interacting Genes in the PPI network. The results demonstrated that 52 nodes and 80 edges were included. (B) Hub genes were identified based on the connectivity of degree, DMNC, MCC and MNC in the PPI network. (C) Venn analysis was performed to identify intersection of DEG profiles, which demonstrated that five genes were overlapping in those four analysis methods. (D) A total of three module networks were analyzed by MCODE, and the most important module with six genes was selected. PPI, protein-protein interaction; DEG, differentially expressed gene; MCODE, Molecular Complex Detection; DMNC, density of maximum neighborhood component; MCC, maximal clique centrality; MNC, mononuclear cell counts.

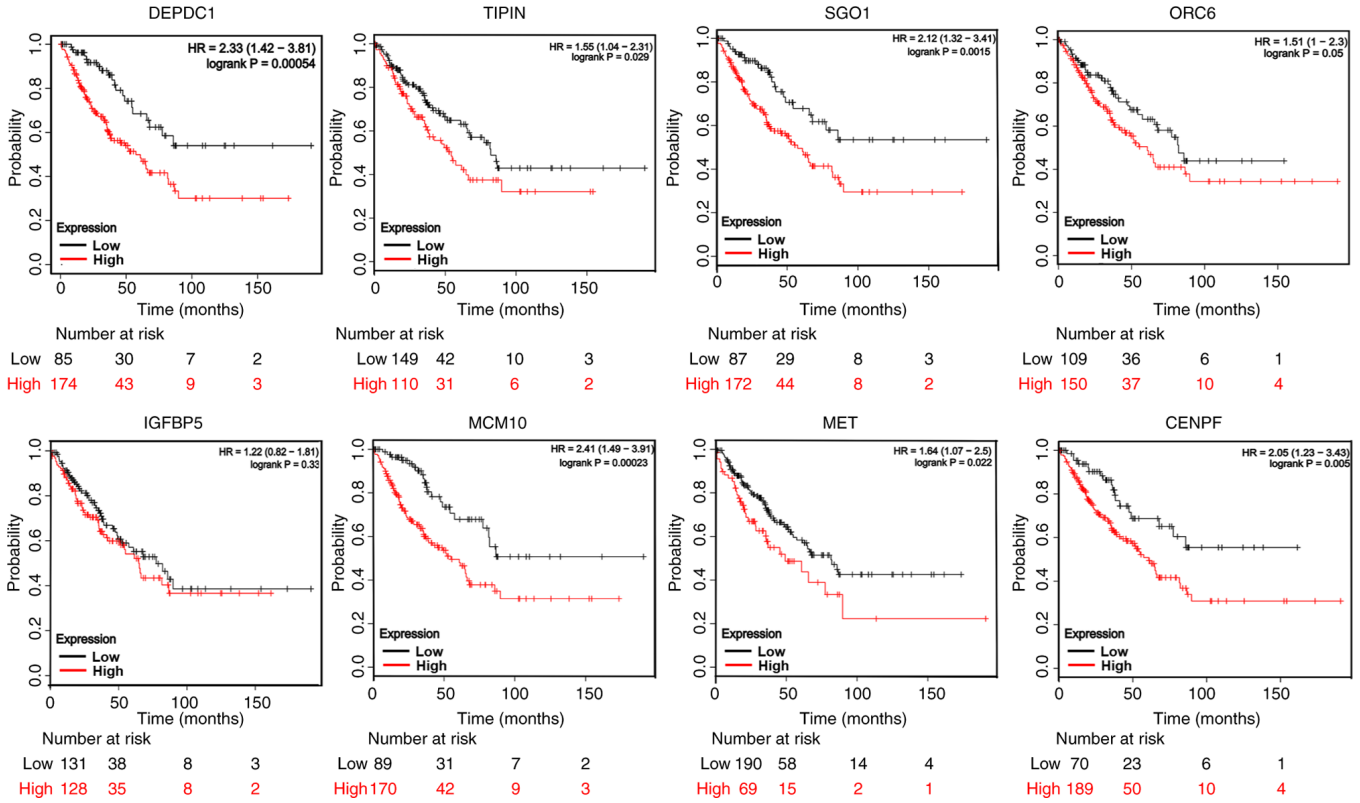

Figure 4. Survival analysis of hub genes. Kaplan-Meier plotter online database revealed the prognostic values of eight hub genes. Overall survival analysis of 259 cases demonstrated that, with the exception of IGFBP5, high expression levels of hub genes (DEPDC1, TIPIN, SGOL1, ORC6, MCM10, MET and CENPF) were associated with an unfavorable overall survival of patients with osteosarcoma. IGFBP5, IGF-binding protein 5; DEPDC1, DEP domain-containing 1; TIPIN, TIMELESS interacting protein; SGOL1, shugoshin 1; ORC6, origin recognition complex subunit 6; MCM10, minichromosome maintenance 10 replication initiation factor; MET, MET proto-oncogene, receptor tyrosine kinase; CENPF, centromere protein F.

collected in Oncomine database, which indicated that IGFBP5 and MET were downregulated in tumor tissues, whereas the other hub genes [DEPDC1, TIPIN, SGOL1(SGO1), ORC6, MCM10 and CENPF] were upregulated in tumor tissues, compared with the adjacent non-tumorous tissues (Fig. 5B). The expression of eight hub genes exhibited a significant difference between tumors and adjacent tissues.

Identification of CENPF transfection efficiency in osteosarcoma cell lines. As aforementioned, ORC6 and CENPF were upregulated in osteosarcoma. Furthermore, Kaplan-Meier plotter indicated that the P-value of CENPF was smaller compared with that of ORC6. Therefore, CENPF was selected for further experiments analyses.

In order to select the most effective siRNA for CENPF, transfection efficiency was assessed using RT-qPCR and western blotting. MG-63 and U-2OS cells were transfected with NC, si-CENPF-1 or si-CENPF-2. The results demonstrated that CENPF expression at both the mRNA and protein levels were significantly downregulated in both cell lines transfected with si-CENPF-2 compared with the NC (*P<0.05, **P<0.01; Fig. 6A-D). Thus, si-CENPF-2 was selected for the following functional experiments.

Knockdown of CENPF suppresses proliferation in osteosarcoma cell lines. In order to analyze the functional role of CENPF in osteosarcoma, CCK-8 assays were performed in MG-63 and U-2OS cell lines. NC and si-CENPF-2 were separately transfected into osteosarcoma cell lines. Proliferation ability was significantly decreased in the si-CENPF-2 group compared with the corresponding NC group (*P<0.05; Fig. 7A and B). This indicated that CENPF knockdown inhibited the proliferation ability of osteosarcoma cell lines.

Knockdown of CENPF decreases migration ability in osteosarcoma cell lines. Wound healing and Transwell migration assays were performed to investigate the effect of CENPF on migration in osteosarcoma cell lines. Cells were transfected with NC and si-CENPF-2 and migration ability was then investigated. In osteosarcoma cell lines, the wound healing rate was significantly decreased in the si-CENPF-2 groups compared with the corresponding NC groups (*P<0.05, **P<0.01; Fig. 8B and D). The results demonstrated that CENPF knockdown decreased migration ability in osteosarcoma cell lines.

Knockdown of CENPF decreases invasion ability in osteosarcoma cell lines. In order to measure invasion ability, Transwell invasion assays were performed in osteosarcoma cell lines using Matrigel-coated Transwell inserts. Cell lines were transfected with NC or si-CENPF-2. The results demonstrated that cells transfected with si-CENPF-2 exhibited significantly lower invasion abilities compared with the corresponding NC groups (**P<0.01, ***P<0.001; Fig. 9). This indicated that downregulated CENPF significantly decreased invasion ability in osteosarcoma cell lines.

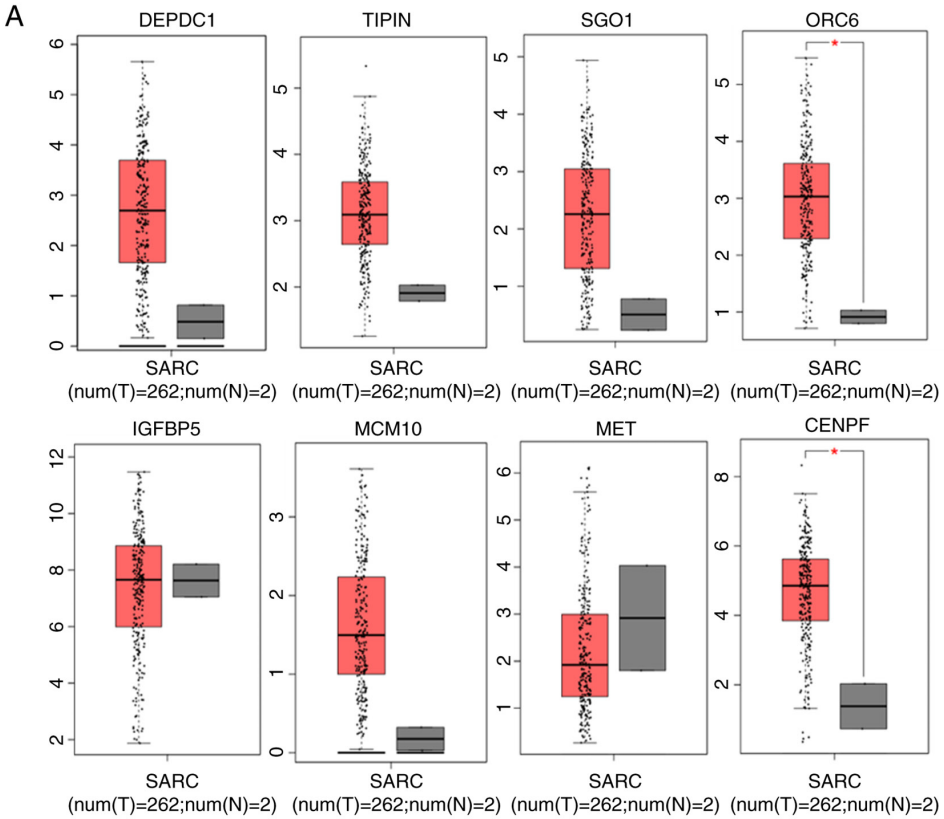

B

Analysis type by cancer	Cancer vs. Normal DEPDC1		Cancer vs. Normal TIPIN		Cancer vs. Normal SGO1		Cancer vs. Normal ORC6		Cancer vs. Normal IGFBP5		Cancer vs. Normal MCM10		Cancer vs. Normal MET		Cancer vs. Normal CENPF	
Bladder cancer										3	2		1		2	
Brain and CNS cancer	1		2	1	1				7		2	1		3	8	
Breast cancer	6		1		3		3	1	1		7			6	14	1
Cervical cancer	1		4				3			1	3		5		3	
Colorectal cancer	8		4		2		13		2		14		20		8	
Esophageal cancer	1		1				1				1		6		1	1
Gastric cancer	2		1		1		2				2		1		4	
Head and neck cancer	1		1							4	2		6		3	
Kidney cancer							4			1			7	1		1
Leukemia		3	1					1		1		1				4
Liver cancer	1										1				2	
Lung cancer	3		2		1		3		3		3				13	
Lymphoma	1								8		2		1		3	
Melanoma										2	2					
Myeloma													1			
Other cancer	4	3	3	4			3	1		1	3		5		1	
Ovarian cancer	2						2			4	1			1	2	
Pancreatic cancer									4				2			
Prostate cancer															1	
Sarcoma	4		1				2			1	4			6	5	
Significant unique analyses	34	6	20	5	8		36	3	25	18	48	2	55	16	69	7
Total unique analyses	375		380		283		369		451		349		441		454	

Figure 5. Confirmation of differential expression hub genes. (A) Gene Expression Profiling Interactive Analysis demonstrated that the hub genes ORC6 and CENPF were upregulated in osteosarcoma (tumor=262; normal=2). *P<0.05. (B) Oncomine database verified that IGFBP5 and MET were downregulated, but the other hub genes (DEPDC1, TIPIN, SGOL1, ORC6, MCM10 and CENPF) were upregulated. SARC, osteosarcoma; T, tumor; N, normal; IGFBP5, IGF-binding protein 5; DEPDC1, DEP domain-containing 1; TIPIN, TIMELESS interacting protein; SGOL1, shugoshin 1; ORC6, origin recognition complex subunit 6; MCM10, minichromosome maintenance 10 replication initiation factor; MET, MET proto-oncogene, receptor tyrosine kinase; CENPF, centromere protein F.

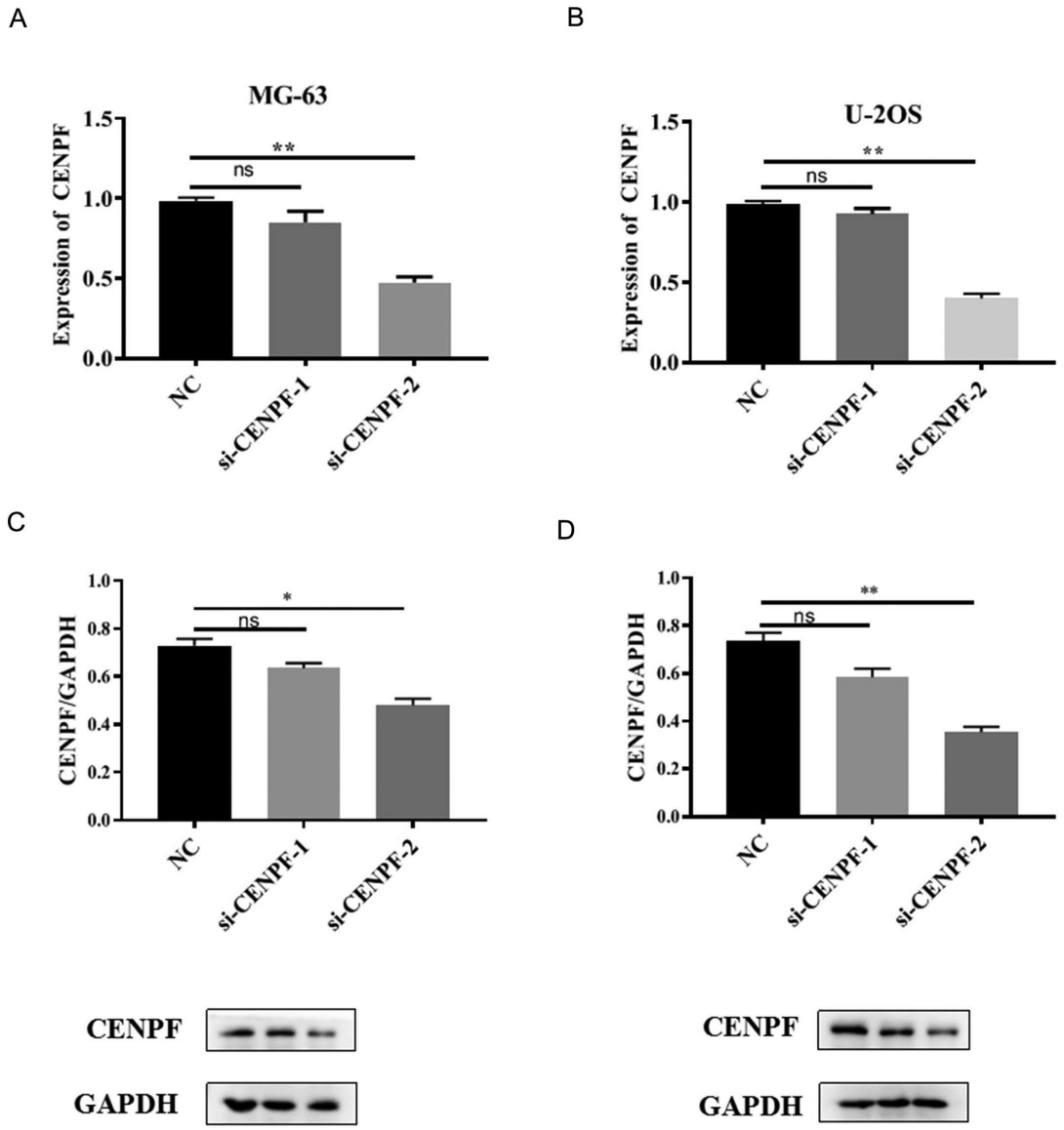

Figure 6. Identification of CENPF transfection efficiency in osteosarcoma cell lines. In order to select the most effective siRNA for CENPF, transfection efficiency was assessed via qPCR and western blotting. Cells were transfected with NC, si-CENPF-1 and si-CENPF-2. mRNA expression levels of CENPF in (A) MG-63 cells and in (B) U-2OS cells transfected with si-CENPF-2 were downregulated. The protein expression levels of CENPF in (C) MG-63 cells and in (D) U-2OS cells transfected with si-CENPF-2 group were downregulated. *P<0.05, **P<0.01. qPCR, quantitative PCR; si, small interfering RNA; CENPF, centromere protein F; NC, negative control; ns, not significant.

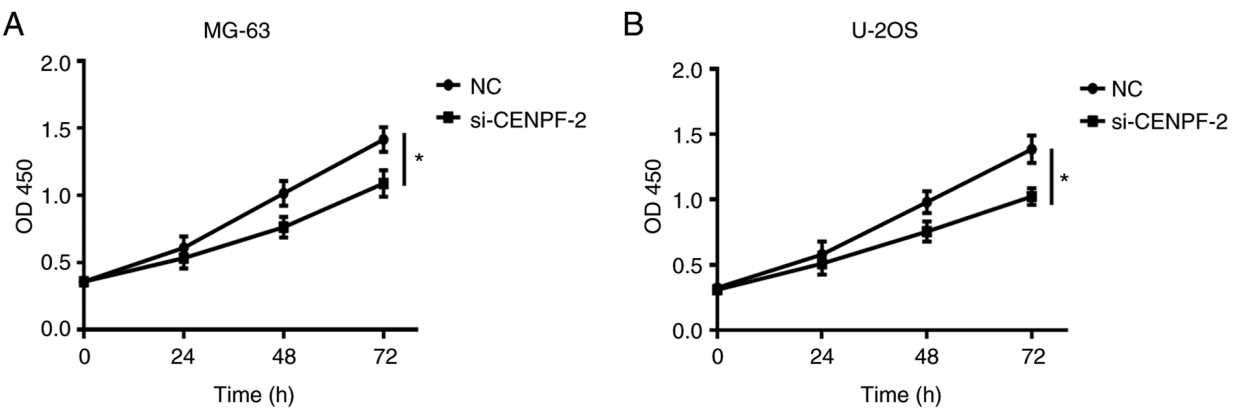

Figure 7. Knockdown of CENPF suppresses proliferation in osteosarcoma cell lines. In order to analyze the functional role of CENPF in osteosarcoma, Cell Counting Kit-8 assays were performed in (A) MG-63 and (B) U-2OS cell lines. NC and si-CENPF-2 were separately transfected into osteosarcoma cell lines. Proliferation ability was decreased in the si-CENPF-2 group compared with the corresponding NC group. *P<0.05. CENPF, centromere protein F; si, small interfering RNA; NC, negative control.

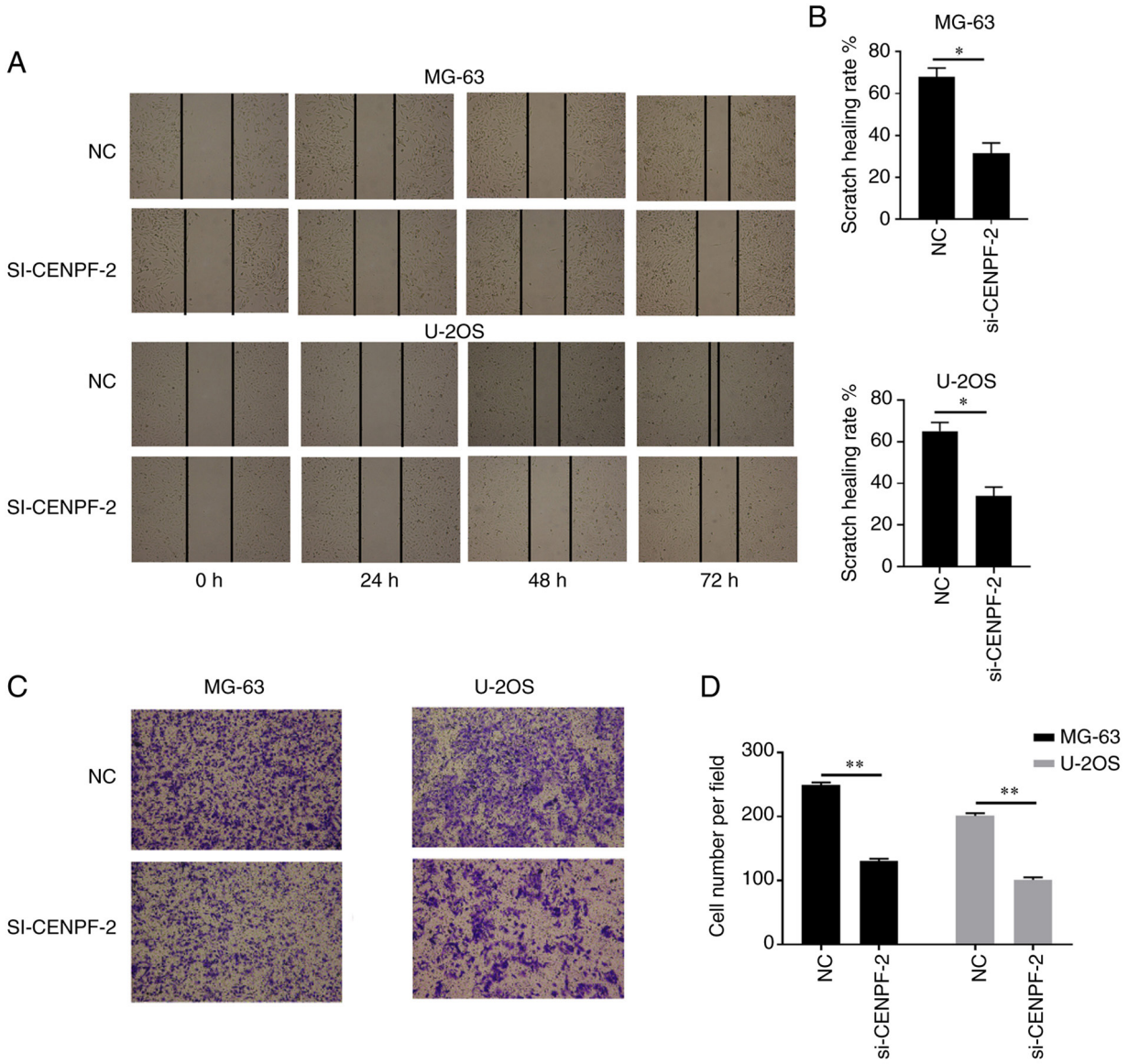

Figure 8. Knockdown of CENPF decreases migration ability in osteosarcoma cell lines. Cells were transfected with NC and si-CENPF-2, and cell migration ability was investigated. (A) Wound healing assays were performed on MG-63 and U-2OS cell lines (magnification, x40), and (B) subsequent quantification revealed that the wound healing rate was decreased in si-CENPF-2 groups compared with their corresponding NC groups. CENPF-knockdown decreased migration ability in osteosarcoma cell lines as detected by (C) Transwell migration assay (magnification, x40) and (D) subsequent quantification. *P<0.05, **P<0.01. CENPF, centromere protein F; si, small interfering RNA; NC, negative control.

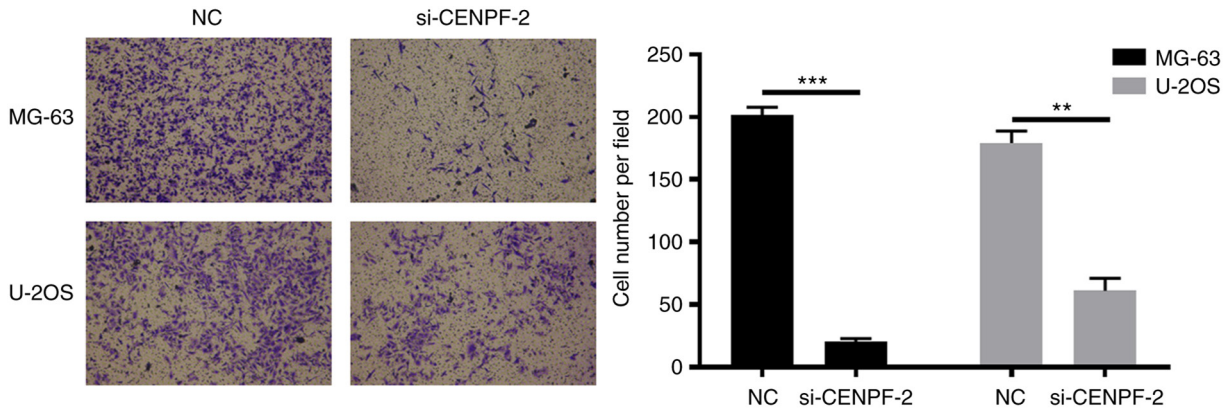

Figure 9. Knockdown of CENPF decreases invasion ability in osteosarcoma cell lines. In order to assess invasion ability, Transwell assays were performed in osteosarcoma cell lines using Matrigel-coated Transwell inserts. Cell lines were transfected with NC and si-CENPF-2. MG-63 and U-2OS cells transfected with si-CENPF-2 exhibited lower invasion ability compared with the NC group. Downregulation of CENPF significantly decreased invasion ability in osteosarcoma cell lines. **P<0.01, ***P<0.001. CENPF, centromere protein F; si, small interfering RNA; NC, negative control.

Discussion

The collection of genomic and clinical information has been commonly used to investigate disease progression and improve medical treatment (31,32). Genomic profiling enables more specific diagnosis and targeted treatment of a number of diseases, including numerous types of cancer (33,34). One method is to obtain bioinformatics information from microarray datasets (35-37). As microarray provides high-throughput experimental data, it can be difficult to elucidate meaningful biological implications from large datasets (38,39). Therefore, the majority of data generated by microarrays are collected in public archives such as GEO (40), Oncomine (41) and The Cancer Genome Atlas (TCGA) (42).

The aforementioned powerful bioinformatics analysis online tools have been widely used for the identification of biomarkers to provide potential therapeutic targets in numerous types of cancer (43): Zhang *et al* (44) investigated miR-146a-5p and its potential targets in hepatocellular carcinoma using TCGA and GEO databases; a study combining data from TCGA, GEO and RT-qPCR determined the clinical value of miR-182-5p in lung squamous cell carcinoma (45); and GEO and TCGA data have been used to investigate the clinical value of the underlying mechanism of ovarian cancer (46). Therefore, it is important to understand how knowledge of genomics can be translated from research into clinical practice, particularly in cancer treatment (47,48).

Osteosarcoma is one of the most common types of primary bone tumor (49) but its etiology is largely unknown (50), which limits understanding and treatment of different cases of osteosarcoma. A growing number of researchers are attempting to capitalize on microarray technology to identify disease-specific molecular signatures and biomarkers for diagnosis, classification and prognosis prediction (51-53). For example, research based on microarray analysis has reported distinct gene expression level profiles associated with histological subtype in human osteosarcoma (54). Zou *et al* (55) identified the frequent expression levels of melanoma antigen protein A and other cancer-testis antigens in osteosarcoma using microarray analysis. Furthermore, microarray analysis has also revealed 48 common genes that are differentially expressed in metastatic cell lines compared with parental cells in metastatic osteosarcoma (56).

The present study used the GEO database to search for potential datasets in order to identify key genes and pathways associated with osteosarcoma. As presented in gene expression level profiles, GSE37552, GSE9508 and GSE19357 were identified. In order to further investigate the statistical significance of DEGs, GO and KEGG analysis indicated that the terms 'regulation of muscle tissue development', 'positive regulation of cell migration', 'bone development' and 'resolution of sister chromatid cohesion' were primarily enriched with DEGs. Subsequently, the PPI network was constructed using the online software STRING. In order to predict the critical genes in osteosarcoma, the top ten genes were identified based on the connectivity of degree, DMNC, MCC and MNC in the PPI network. Venn analysis was performed to determine the intersection of the DEG profiles, which demonstrated that five genes were overlapping in those four analysis methods. In addition, MCODE analysis indicated that six key genes exhibited strong interactions. Combined with the results of PPI network construction and MCODE analyses, eight hub genes were obtained (DEPDC1, TIPIN, SGOL1, ORC6, IGFBP5, MCM10, MET and CENPF). Furthermore, Kaplan-Meier survival analysis was performed to identify the prognostic value of these eight hub genes. The results indicated that overexpression of seven hub genes (DEPDC1, TIPIN, SGOL1, ORC6, MCM10, CENPF and MET) was associated with less favorable overall survival in patients with osteosarcoma. GEPIA and Oncomine databases were used to confirm differential hub gene expression levels in tissue. The hub gene CENPF was selected for further experiments to determine its effects on the proliferative, migratory and invasive abilities of osteosarcoma cells. CCK-8, wound healing and Transwell migration and invasion assays results indicated that CENPF knockdown inhibited the proliferation, migration and invasion of osteosarcoma cell lines. However, further investigation is required to identify potential causes.

The present study screened three gene expression level profiles to select DEGs, and then performed functional enrichment analyses of DEGs using GO and KEGG. Potential associated factors involved in osteosarcoma were identified. Moreover, PPI network construction and MCODE analyses were conducted, and seven novel genes associated with osteosarcoma were identified. In order to determine the prognostic value of these genes, the Kaplan-Meier method was used for overall survival analysis. GEPIA and Oncomine further confirmed expression levels of hub genes. The functional experiments demonstrated that knockdown of the hub gene CENPF inhibited proliferation, migration and invasion in osteosarcoma cell lines. These results may indicate targets for novel therapeutic strategies for osteosarcoma.

Acknowledgements

Not applicable.

Funding

The present study was supported by Wuhan Young and Middle-aged Medical Backbone Talents.

Availability of data and materials

The datasets used and/or analyzed during the current study are available from the corresponding author on reasonable request.

Authors' contributions

YM contributed to the conception and design of the present study. YM and JG analyzed and interpreted the results, and wrote the manuscript. DL and XC performed the experiments. DL and XC confirm the authenticity of all the raw data. All authors have read and approved the final manuscript.

Ethics approval and consent to participate

Not applicable.

Patient consent for publication

Not applicable.

Competing interests

The authors declare that they have no competing interests.

References

1. Kong C and Hansen MF: Biomarkers in osteosarcoma. Expert Opin Med Diagn 3: 13-23, 2009.
2. Ottaviani G and Jaffe N: The epidemiology of osteosarcoma. Cancer Treat Res 152: 3-13, 2009.
3. Neyssa M, Mark G, Lisa T and Richard G: Biology and therapeutic advances for pediatric osteosarcoma. Oncologist 9: 422-421, 2004.
4. Machak GN, Tkachev SI, Solovyev YN, Sinyukov PA, Ivanov SM, Kochergina NV, Ryjkov AD, Tepliakov VV, Bokhian BY and Glebovskaya VV: Neoadjuvant chemotherapy and local radiotherapy for high-grade osteosarcoma of the extremities. Mayo Clin Proc 78: 147-155, 2003.
5. Kaya M, Wada T, Akatsuka T, Kawaguchi S, Nagoya S, Shindoh M, Higashino F, Mezawa F, Okada F and Ishii S: Vascular endothelial growth factor expression in untreated osteosarcoma is predictive of pulmonary metastasis and poor prognosis. Clin Cancer Res 6: 572-577, 2000.
6. Picci P, Vanel D, Briccoli A, Talle K, Haakenaasen U, Malaguti C, Monti C, Ferrari C, Bacci G, Saeter G and Alvegard TA: Computed tomography of pulmonary metastases from osteosarcoma: The less poor technique. A study of 51 patients with histological correlation. Ann Oncol 12: 1601-1604, 2001.
7. Li W, Xie P and Ruan WH: Overexpression of lncRNA UCA1 promotes osteosarcoma progression and correlates with poor prognosis. J Bone Oncol 5: 80-85, 2016.
8. Wei L, Peng X and Wen-Hui R: Overexpression of lncRNA UCA1 promotes osteosarcoma progression and correlates with poor prognosis. J Bone Oncol 5: 80-85, 2016.
9. Zhao H, Hou W, Tao J, Zhao Y, Wan G, Ma C and Xu H: Upregulation of lncRNA HNF1A-AS1 promotes cell proliferation and metastasis in osteosarcoma through activation of the Wnt/β-catenin signaling pathway. Am J Transl Res 8: 3503-3512, 2016.
10. Zhang CL, Zhu KP and Ma XL: Antisense lncRNA FOXC2-AS1 promotes doxorubicin resistance in osteosarcoma by increasing the expression of FOXC2. Cancer Lett 396: 66-75, 2017.
11. Zhang F and Peng H: LncRNA-ANCR regulates the cell growth of osteosarcoma by interacting with EZH2 and affecting the expression of p21 and p27. J Orthop Surg Res 12: 103, 2017.
12. Peng ZQ, Lu RB, Xiao DM and Xiao ZM: Increased expression of the lncRNA BANCR and its prognostic significance in human osteosarcoma. Genetics Mol Res: doi: 10.4238/gmr.15017480, 2016.
13. Edgar R, Domrachev M and Lash EA: Gene expression omnibus: NCBI gene expression and hybridization array data repository. Nucleic Acids Res 30: 207-210, 2002.
14. Tan Q, Thomassen M, Jochumsen KM, Zhao JH, Christensen K and Kruse TA: Evolutionary algorithm for feature subset selection in predicting tumor outcomes using microarray data. In: Bioinformatics Research and Applications. ISBRA 2008. Lecture Notes in Computer Science. Vol 4983. Măndoiu I, Sunderraman R and Zelikovsky A (eds). Springer, Berlin, Heidelberg, 2008.
15. Shen R, Ghosh D, Chinnaiyan A and Meng Z: Eigengene-based linear discriminant model for tumor classification using gene expression microarray data. Bioinformatics 22: 2635-2642, 2006.
16. Kannan S and Neelapu S: Abstract #1434: Meta-analysis of multiple Follicular Lymphoma GEO datasets reveals the significance of tumor microenvironment in disease progression. Cancer Res 69, 1434, 2009.
17. Li Q, Smith AJ, Schacker TW, Carlis JV, Duan L, Reilly CS and Haase AT: Microarray analysis of lymphatic tissue reveals stage-specific, gene expression signatures in HIV-1 infection. J Immunol 183: 1975-1982, 2015.
18. Kampas D, Soulitzis N, Neofytou E and Siafakas NM: Microarray cluster analysis reveals individual genes and biological processes associated with COPD. Eur Respir J 44: P3821, 2014.
19. Li CY, Pang YY, Yang H, Li J, Lu HX, Wang HL, Mo WJ, Huang LS, Feng ZB and Chen G: Identification of miR-101-3p targets and functional features based on bioinformatics, meta-analysis and experimental verification in hepatocellular carcinoma. Am J Transl Res 9: 2088-2105, 2017.
20. Zhou Z, Li Y, Hao H, Wang Y, Zhou Z, Wang Z and Chu X: Screening hub genes as prognostic biomarkers of hepatocellular carcinoma by bioinformatics analysis. Cell Transplant 28 (1_Suppl): 76S-86S, 2019.
21. Cuff J, Salari K, Clarke N, Esheba GE, Forster AD, Huang S, West RB, Higgins JP, Longacre TA and Pollack JR: Integrative bioinformatics links HNF1B with clear cell carcinoma and tumor-associated thrombosis. PLoS One 8: e74562, 2013.
22. Yu Z, Chen WJ, Gan TQ, Zhang XL, Xie ZC, Ye ZH, Deng Y, Wang ZF, Cai KT, Li SK, *et al*: Clinical significance and effect of lncRNA HOXA11-AS in NSCLC: A study based on bioinformatics, *in vitro* and *in vivo* verification. Sci Rep 7: 5567, 2017.
23. Flores RJ, Li Y, Yu A, Shen J, Rao PH, Lau SS, Vannucci M, Lau CC and Man TK: A systems biology approach reveals common metastatic pathways in osteosarcoma. BMC Syst Biol 6: 50, 2012.
24. Endo-Munoz L, Cumming A, Rickwood D, Wilson D, Cueva C, Ng C, Strutton G, Cassady AI, Evdokiou A, Sommerville S, *et al*: Loss of osteoclasts contributes to development of osteosarcoma pulmonary metastases. Cancer Res 70: 7063-7072, 2010.
25. Sun C, Yuan Q, Wu D, Meng X and Wang B: Identification of core genes and outcome in gastric cancer using bioinformatics analysis. Oncotarget 8: 70271-70280, 2017.
26. Gene Ontology Consortium: The gene ontology (GO) project in 2006. Nucleic Acids Res 34: D322-D326, 2006.
27. Kanehisa M and Goto S: KEGG: Kyoto encyclopedia of genes and genomes. Nucleic Acids Res 28: 27-30, 2000.
28. Chin CH, Chen SH, Wu HH, Ho CW, Ko MT and Lin CY: CytoHubba: Identifying hub objects and sub-networks from complex interactome. BMC Syst Biol 8 Suppl 4 (Suppl 4): S11, 2014.
29. Bader GD and Hogue CW: An automated method for finding molecular complexes in large protein interaction networks. BMC Bioinformatics 4: 2, 2003.
30. Livak KJ and Schmittgen TD: Analysis of relative gene expression data using real-time quantitative PCR and the 2(-Delta Delta C(T)) method. Methods 25: 402-408, 2001.
31. Jiang X, Barmada MM and Visweswaran S: Identifying genetic interactions in genome-wide data using Bayesian networks. Genet Epidemiol 34: 575-581, 2010.
32. De Backer MD, Ilyina T, Ma XJ, Vandoninck S, Luyten WH and Bossche HV: Genomic profiling of the response of candida albicans to itraconazole treatment using a DNA microarray. Antimicrob Agents Chemother 45: 1660-1670, 2001.
33. Mirshahidi HR and Abraham J: Genomic profiling in clinical oncology. The predictive value of genomic information in cancer management. Postgrad Med 119: 56-61, 2006.
34. Wulfkuhle J, Espina V, Liotta L and Petricoin E: Genomic and proteomic technologies for individualisation and improvement of cancer treatment. Eur J Cancer 40: 2623-2632, 2004.
35. Stuart JM, Eran S, Daphne K and Kim SK: A gene-coexpression network for global discovery of conserved genetic modules. Science 302: 249-255, 2003.
36. Tsuyuzaki K, Tominaga D, Kwon Y and Miyazaki S: Two-way AIC: Detection of differentially expressed genes from large scale microarray meta-dataset. BMC Genomics 14 (Suppl 2): S9, 2013.
37. Jeyachidra J and Punithavalli M (eds): A comparative analysis of feature selection algorithms on classification of gene microarray dataset. In: 2013 International Conference on Information Communication and Embedded Systems (ICICES), pp1088-1093, 2013. doi: 10.1109/ICICES.2013.6508165.
38. Magnan CN, Zeller M, Kayala MA, Vigil A, Randall A, Felgner PL and Baldi P: High-throughput prediction of protein antigenicity using protein microarray data. Bioinformatics 26: 2936-2943, 2010.
39. Alonso-Betanzos A and Herrera F: A review of microarray datasets and applied feature selection methods. Inf Sci 282: 111-135, 2014.
40. Barrett T, Wilhite SE, Ledoux P, Evangelista C, Kim IF, Tomashevsky M, Marshall KA, Phillippy KH, Sherman PM, Holko M, *et al*: NCBI GEO: Archive for functional genomics data sets-update. Nucleic Acids Res 41: D991-D995, 2013.
41. Rhodes DR, Yu J, Shanker K, Deshpande N, Varambally R, Ghosh D, Barrette T, Pandey A and Chinnaiyan AM: ONCOMINE: A cancer microarray database and integrated data-mining platform. Neoplasia 6: 1-6, 2004.

42. Tomczak K, Czerwińska P and Wiznerowicz M: The cancer genome atlas (TCGA): An immeasurable source of knowledge. Contemp Oncol (Pozn) 19: A68-A77, 2015.
43. Tao Z, Shi A, Li R, Wang Y, Wang X and Zhao J: Microarray bioinformatics in cancer- a review. J BUON 22: 838-843, 2017.
44. Zhang X, Ye ZH, Liang HW, Ren FH, Li P, Dang YW and Chen G: Down-regulation of miR-146a-5p and its potential targets in hepatocellular carcinoma validated by a TCGA- and GEO-based study. FEBS Open Bio 7: 504-521, 2017.
45. Luo J, Shi K, Yin SY, Tang RX, Chen WJ, Huang LZ, Gan TQ, Cai ZW and Chen G: Clinical value of miR-182-5p in lung squamous cell carcinoma: A study combining data from TCGA, GEO, and RT-qPCR validation. World J Surg Oncol 16: 76, 2018.
46. Li XJ, Pang JS, Li YM, Ahmed FA, He RQ, Ma J, Ma FC and Chen G: Clinical value of survivin and its underlying mechanism in ovarian cancer: A bioinformatics study based on GEO and TCGA data mining. Pathol Res Pract 214: 385-401, 2018.
47. Phillips KA, Liang SY, Bebber SV; Canpers Research Group: Challenges to the translation of genomic information into clinical practice and health policy: Utilization, preferences, and economic value. Curr Opin Mol Ther 10: 260-266, 2008.
48. Arao T, Matsumoto K, Maegawa M and Nishio K: What can and cannot be done using a microarray analysis? Treatment stratification and clinical applications in oncology. Biol Pharm Bull 34: 1789-1793, 2011.
49. Alleyne CH, Theodore N, Spetzler RF and Coons SW: Osteosarcoma of the temporal fossa with hemorrhagic presentation: Case report. Neurosurgery 47: 450-451, 2000.
50. Fuchs B and Pritchard DJ: Etiology of osteosarcoma. Clin Orthop Relat Res 397: 40-52, 2002.
51. Heller MJ: DNA microarray technology: Devices, systems, and applications. Annu Rev Biomed Eng 4: 129-153, 2002.
52. Statnikov A, Aliferis CF, Tsamardinos I, Hardin D and Levy S: A comprehensive evaluation of multicategory classification methods for microarray gene expression cancer diagnosis. Bioinformatics 21: 631-643, 2005.
53. Gevaert O and Moor BD: Prediction of cancer outcome using DNA microarray technology: Past, present and future. Expert Opin Med Diagn 3: 157-165, 2009.
54. Kubista B, Klinglmueller F, Bilban M, Pfeiffer M, Lass R, Giurea A, Funovics PT, Toma C, Dominkus M, Kotz R, *et al*: Microarray analysis identifies distinct gene expression profiles associated with histological subtype in human osteosarcoma. Int Orthop 35: 401-411, 2011.
55. Zou C, Shen J, Tang Q, Yang Z, Yin J, Li Z, Xie X, Huang G, Lev D and Wang J: Cancer-testis antigens expressed in osteosarcoma identified by gene microarray correlate with a poor patient prognosis. Cancer 118: 1845-1855, 2012.
56. Muff R, Kumar RMR, Botter SM, Born W and Fuchs B: Genes regulated in metastatic osteosarcoma: Evaluation by microarray analysis in four human and two mouse cell line systems. Sarcoma 2012: 937506, 2012.